JOURNAL OF CATALYSIS **83**, 286–300 (1983)

Conversion of Isobutane over Solid Acids—A Sensitive Mechanistic Probe Reaction

G. B. McVicker, G. M. Kramer, and J. J. Ziemiak

Exxon Research and Engineering Company, Corporate Research Laboratories, Linden, New Jersey 07036

Received January 14, 1983; revised May 10, 1983

Amorphous solid acids, such as SiO_2–Al_2O_3 and halided-Al_2O_3, convert isobutane at elevated temperatures (700–920 K) to a limited number of products. These solid acids crack isobutane 30 to 400 times faster than a blank reactor, and yield a product consisting primarily of methane, propene, butenes, and hydrogen. This product distribution is similar to that obtained thermally. Conversion rates over amorphous solid acids display a first-order isobutane pressure dependency. In contrast to amorphous solid acids, a highly active, ultrastable Y, faujasite exhibits a paraffinic rather than an olefinic product. Hydrogen is not produced in significant quantities over faujasite but is incorporated into the conversion products. Isomerization to *n*-butane is a major path, rather than a trace reaction, alkylation reactions yielding $C_5(+)$ hydrocarbons readily occur and methane production is reduced. The rates of formation of cracking fragments, *n*-butane, and $C_5(+)$ products are second-order in isobutane. The product distribution and kinetics lead to the conclusion that amorphous solid acids convert isobutane by a different mechanism than faujasite. Over amorphous solid acids, the data are not consistent with the presence of "free" carbonium ion intermediates whereas with faujasite it is. Radical cations are suggested as initial intermediates over all solid acid systems and differences in their subsequent reactions account for the observed variation in products and kinetic orders.

1. INTRODUCTION

Recent studies in these laboratories have established that the conversion of isobutane over solid acids is a sensitive mechanistic probe reaction. Detailed analyses of isobutane isomerization and cracking patterns have enabled us to ascertain the relative contributions of carbonium ion and radical processes occurring on solid acids at temperatures typically employed in catalytic cracking (*1*, *2*).

Although a simple molecule, isobutane yields a sizable number of products when subjected to high (670–920 K) temperatures. Figure 1 outlines the major reaction products expected from carbonium ion and free-radical (or radical cation) intermediates. The significantly different slate of products can be used to identify the preferred pathway by which isobutane is converted over a wide range of solid acids. Well-developed theories of organic chemistry predict the following products from carbonium ion initiated reactions of isobutane: *n*-butane, butenes at or near equilibrium concentrations, and a paraffinic C_2–C_3 crackate and $C_5(+)$ alkylate (*3*, *4*). Tertiary and secondary C_4 carbonium ions are not expected to crack by conventional β-scission pathways (*5*). The predicted C_2–C_3 crackate and $C_5(+)$ products can, however, arise from a polymerization–rearrangement–cracking sequence of reactions (*6*, *7*). The C_2–C_3 crackate and $C_5(+)$ products may be paraffinic as a consequence of intermolecular hydride transfer reactions. Methane is not expected from a carbonium ion assisted decomposition route.

At temperatures above about 700 K, radical initiated cracking processes become important (*8*–*10*). The homolytic rupture of any of the equivalent carbon–carbon bonds of isobutane would ultimately yield equimolar quantities of methane and propene as primary products. The most favorable carbon–hydrogen bond cleavage occurs at the tertiary carbon atom (*11*). Homolytic cleav-

0021-9517/83 $3.00

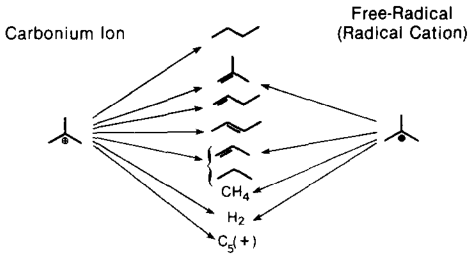

FIG. 1. Major isobutane conversion products expected from carbonium ion and radical intermediates.

age of this bond would lead to isobutene and hydrogen as primary products. No isomerization of the primary isobutene product is expected. Radical intermediates such as $CH_3^{\cdot}$ and $C_4H_9^{\cdot}$ can couple to form $C_5(+)$ products. Coupling products may become important if the radical concentration is high and the cracking temperature remains low (*10, 12*). At the elevated temperatures employed here, however, the major products are anticipated to be methane, propene, isobutene, and hydrogen. Similar products are expected from the unimolecular decomposition of a radical cation intermediate (*13*). An isobutane radical cation, $C_4H_{10}^{\ddagger}$, produced by the one electron oxidation of isobutane, undergoes facile elimination reactions yielding the pairwise products isobutene and hydrogen and propene and methane (*14–16*).

At the start of these studies, the parameters listed in Table 1 were anticipated to provide a means of ranking the acid strengths of solid acids. A total of 10 solid acids were investigated over a wide range of conversion temperatures. These included nine amorphous (or microcrystalline) solid acids, namely, silica–alumina, alumina, and a series of halided-alumina catalysts and one crystalline faujasite catalyst. These solid acids were selected, since they are generally accepted to represent a wide range of acid strengths (*17*). Only the faujasite catalyst was found to exhibit appreciable carbonium ion type reactivity. Thus, the parameters listed in Table 1 could not be used to scale the acidities of these particular acids. The present studies have, however, shown that as a class solid acids catalyze the radical-like cracking of isobutane. In the specific case of the faujasite catalyst, olefins generated by a radical-like cracking reaction subsequently undergo carbonium ion initiated conversions. This paper experimentally verifies the often cited conjecture (*18, 19*) that radical-like and carbonium ion processes can simultaneously take place on the surface of solid acids during the isomerization of paraffinic molecules.

TABLE 1

Key Selectivity Parameters

Parameter	Expected trends
$\frac{C_1}{C_1\text{–}C_3}$	Decreases with increasing acidity; a value of 0.50 reflects radical cracking
$\frac{n\text{–}C_4}{C_1\text{–}C_3}$	Increases with increasing acidity
$\frac{C_3}{C_3^{=}}$	Increases with increasing acidity as a result of enhanced hydride transfer

2. EXPERIMENTAL SECTION

Catalysts

SiO_2–Al_2O_3. The amorphous silica–alumina catalyst used in these studies was a commercial sample obtained from the Davison Chemical Company. The catalyst contains 87 wt% SiO_2 and 13 wt% Al_2O_3. The BET surface area of the material measured 350 m^2/g (*20*).

γ-Al_2O_3. A reforming grade γ-Al_2O_3, supplied by Engelhard Minerals and Chemicals Corporation, was employed throughout these studies and exhibited a BET surface area of 178 m^2/g.

Halided-Al_2O_3. Chlorided and fluorided-alumina catalysts (0.3 to 5 wt% halide) were prepared by impregnation of γ-Al_2O_3 with standardized aqueous HCl and HF solutions. The wet impregnates were dried at

393 K for 16 hr and then calcined at 773 K for 4 hr under air. Halide analyses were performed by the Analytical and Information Division, Exxon Research and Engineering Company, Linden, New Jersey. The halided samples exhibited BET surface areas in the range 170–185 m^2/g and displayed X-ray diffraction patterns indistinguishable from that of γ-Al_2O_3.

Faujasite. The ultrastable Y zeolite used throughout these studies was obtained from the Linde Company. Linde designates the material LZ-Y82 and supplied the following analyses (wt%): SiO_2 (72.2), Al_2O_3 (22.8), and Na_2O (0.2). The zeolite is in its hydrogen form and exhibits a BET surface area of 770 m^2/g.

$MgAl_2O_4$. A nonacidic magnesium aluminate catalyst was synthesized by S. L. Soled of our laboratories. The material crystallizes in a spinel structure isomorphous with γ-Al_2O_3 and exhibits a BET surface area of 155 m^2/g.

Catalytic Conversions

Isobutane conversions were carried out at 101 kPa total pressure in a 22 cm^3, stainless-steel, fixed-bed reactor operated once through. The reactor was heated by a Lindberg electrical furnace. Isobutane and helium (carrier) gases were metered separately and were well blended prior to admission to the reactor. A standard reactor bed configuration consisting of a 2 cm^3 preheat zone (mullite, 10/16 mesh), a catalyst zone containing 1.0 g of catalyst (2–3 cm^3, 10/20 mesh) diluted to 18 cm^3 with mullite beads and finally a postreactor zone containing 2 cm^3 of mullite beads was employed in all studies. Catalyst zone temperature was monitored by a movable thermocouple normally placed at the mid-point of the bed. The start-up procedure for each sample consisted of drying the catalyst at 773 K for 1.0 hr under dry helium flowing at 400 cm^3/min. Reaction products exited the reactor via heated lines and were analyzed by on-line GC measurements. A Varian 3700 gas chromatograph employing flame ionization detection and equipped with a 50-m fused silica capillary column coated with SP-2100, allowed excellent product separation and identification.

Normal Operating Procedure

Following pretreatment, the helium flow was set at 150 cm^3/min at the desired starting temperature. After achieving thermal equilibrium, 50 cm^3/min of isobutane was added to the helium carrier stream (25.3 kPa isobutane). After 10 min on feed, a GC sample was taken and the isobutane flow was stopped. While maintaining the helium flow (150 cm^3/min) the reactor temperature was adjusted to the next set-point. Generally, about 45 min was required to establish the new temperature. Isobutane was then reintroduced for a second 10-min period, following which a GC sample was taken. Routinely seven to nine different temperatures were employed per each run. The set-points were established in both ascending and descending temperature sequences.

Added Oxygen Studies

The effect of oxygen on the catalytic conversion of isobutane was investigated by employing a 0.1% O_2/He mixture in place of the normal helium-only carrier gas.

Added Water Studies

The effect of water on the catalytic conversion of isobutane was studied by passing the isobutane/helium mixture (200 cm^3/min) through two water saturators maintained at 0°C. The resultant water partial pressure was 0.61 kPa.

Isobutane Partial Pressure Studies

The effect of isobutane partial pressure on conversion patterns was investigated at 12.6, 25.3, and 50.5 kPa of isobutane. To ensure a constant residence time within the reactor, the total flow rate was held at 200 cm^3/min by varying the helium flow rate.

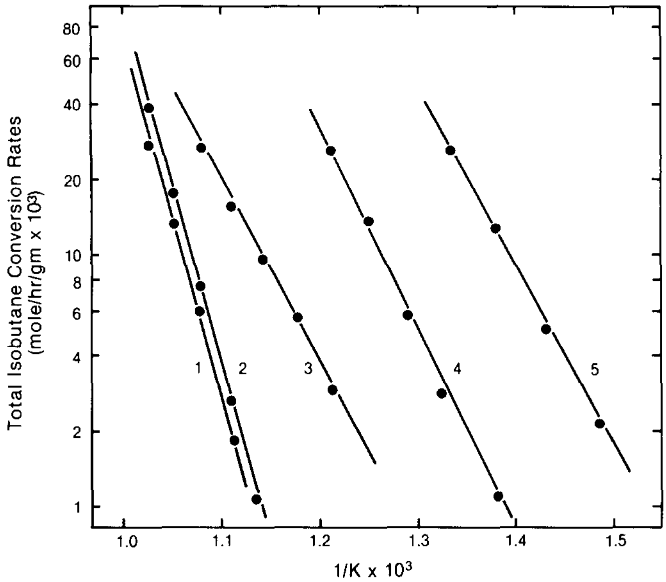

FIG. 2. Arrhenius plots for the conversion of isobutane over selected solid acids. Reaction conditions: 101 kPa total pressure, 50 cm^3 i-C_4H_{10}/min, 150 cm^3 He/min, 1.0 g catalyst. (1) Blank (*59*), (2) $MgAl_2O_4$ (*62*), (3) SiO_2–Al_2O_3 (*33*), (4) 0.9% F–Al_2O_3 (*39*), (5) faujasite (*35*). Apparent activation energies (kcal/mole) in brackets.

Reaction Rates

Reaction rates for selected isobutane conversion reactions were calculated (*21*) using the expression:

$$\text{rate} = \frac{F\Delta X}{W}$$

where F is the isobutane feed rate in moles per hour, W is the weight of catalyst in grams, and ΔX is the extent of isobutane conversion to a particular product. Plots of isobutane conversion against reciprocal space velocity were linear up to 40–50% conversion. Thus, the use of the above expression was judged to adequately describe the present system over a wide range of conversions.

Acidity Measurements

The acidity of the solid acids employed in these studies was characterized by ammonia, 2,6-dimethylpyridine, and 3,5-dimethylpyridine adsorption measurements. The quantity of base adsorbed at 523K was ascertained by TG measurements using a Mettler TA2000C apparatus. The details of the TG procedure used have been described elsewhere (*22*).

3. RESULTS AND DISCUSSIONS

Comparison of Isobutane Conversion Rates

Arrhenius plots for the conversion of isobutane over several representative solid acids are shown in Fig. 2. Negligible deactivation was observed, as conversion rates measured in an ascending temperature sequence were reproduced within 5% in a subsequent descending temperature sequence. Catalysts accumulate less than 1 wt% coke during the course of each run. This corresponds to less than 0.1% of the available feed carbon ending up as coke on catalyst. The low coke makes are an experimental plus, since catalyst comparisons in the absence of significant catalyst deactivation can be made.

A blank reactor (reactor filled with mullite beads) and a nonacidic $MgAl_2O_4$ catalyst exhibit low conversion rates and appar-

TABLE 2

Conversion of Isobutane over Amorphous Solid Acids[a]

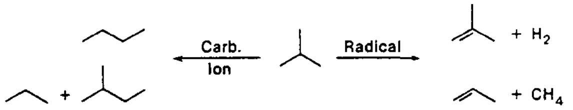

Products (mole%)	Catalyst					
	Blank	$MgAl_2O_4$	γ-Al_2O_3	SiO_2–Al_2O_3	0.9% Cl–Al_2O_3	0.9% F–Al_2O_3
(T °K)	923	923	873	873	873	823
Methane	1.6	1.4	1.6	1.5	8.1	7.3
Propene	1.8	1.5	1.4	1.7	7.4	7.0
Butenes	2.5	4.0	4.2	4.9	7.6	9.0
Propane	—	—	—	0.1	0.1	0.6
n-Butane	—	—	—	0.2	tr	0.3
Pentanes	—	—	—	—	—	tr
i-Butane	94.0	93.0	92.6	91.4	76.0	74.7
Minor	0.1	0.1	0.2	0.2	0.8	1.1
H/C ratio	2.19	2.21	2.13	2.12	2.25	2.22

[a] Reaction conditions: 101 kPa total pressure, 50 cm^3 *i*-C_4H_{10}/min, 150 cm^3 He/min, 1.0 g catalyst.

ent activation energies of about 60 kcal/mole. These activation energies are consistent with those reported for the thermal (free-radical) decomposition of a variety of paraffinic hydrocarbons (*10*, *23*). SiO_2–Al_2O_3 and 0.9% F–Al_2O_3 displayed substantially higher conversion rates and lower apparent activation energies than the blank reactor. The measured activation energies agree with those reported for the cracking of paraffins over amorphous SiO_2–Al_2O_3 catalysts (*24*, *25*). Of the solid acid catalysts tested, the faujasite catalyst demonstrated the highest isobutane conversion rates. The apparent activation energy of 35 kcal/mole exhibited by faujasite is comparable to literature values for the cracking of numerous hydrocarbons over zeolites (*26–28*). A measure of the relative activities of these solid acid catalysts can be made by comparing the temperatures required to establish a given conversion rate. At a conversion rate of 0.01 mole/hr/g, reaction temperatures ranged from 940 K for the blank reactor to 710 K for faujasite. A more quantitative description of the relative activities of these and other solid acids will be made in a later section.

Comparison of Product Distributions

The major isobutane conversion products (hydrogen free basis) displayed by a blank reactor and a number of solid acids are summarized in Table 2. The products have been grouped to highlight those expected from radical and carbonium ion conversion processes. To minimize the generation of secondary reaction products, reaction temperatures were selected to limit conversion to 25% or less. The blank reactor and $MgAl_2O_4$ exhibited an identical set of products with the major components being methane, propene, and isobutene. Minor products, amounting to less than 2% of the total product slate, consisted of ethene and C_6–C_8 aromatics. No isomerization of isobutane to *n*-butane occurred in either run. The C_3 fraction contains only propene and the C_1/C_1–C_3 mole ratio is near 0.5. These results indicate the direct cleavage of isobutane into methane and propene and the absence of secondary hydride-transfer reactions. The generation of essentially equimolar concentrations of isobutene and hydrogen was established by mass spectrometer measurements. The production of hydrogen is reflected in the low H/C ratio of the product molecules (the H/C of isobutane is 2.5). No isomerization of the primary isobutene product occurred over either the blank reactor or the nonacidic $MgAl_2O_4$ catalyst. Conversion products obtained with either a blank reactor or $MgAl_2O_4$ agree completely with those expected for the free-radical cracking of isobutane.

As found using a blank reactor, the major conversion products exhibited by SiO_2–Al_2O_3, γ-Al_2O_3, and halided-Al_2O_3 are methane, propene, and butenes. These components account for over 95% of the hydrocarbon products generated by these acids. Minor products are comprised primarily of ethene and C_6–C_8 aromatics. The essentially exclusive production of methane, propene, and butenes indicates that amorphous solid acids crack isobutane by a radical-like mechanism. For a given conversion level, however, amorphous solid acids require 50 to 150 K lower reaction temperatures than the blank reactor. The lower temperature requirements indicate that amorphous solid acids catalyze the radical-like decomposition of isobutane. This is an unexpected finding, since radical cracking of paraffins is generally accepted to be a homogeneous gas phase reaction. The catalysis of radical-like cracking suggests that solid acids generate and possibly stabilize radical-like species on their surface.

SiO_2–Al_2O_3 and 0.9% F-Al_2O_3 exhibited limited abilities to isomerize isobutane to *n*-butane. At 873 K, *n*-butane selectivities of only 1 to 2% were exhibited by these catalysts. In contrast to the blank reactor or the nonacidic $MgAl_2O_4$ catalyst, amorphous solid acids generate butenes in near equilibrium concentrations (see Table 3). Thus, amorphous solid acids readily isomerize butenes but not butanes. General expressions for the isomerization of isobutane and isobutene are summarized in Eqs. (1) and (2). If free carbonium ion intermediates are involved in the isomerization of butanes and butenes, Eqs. (1) and (2) suggest that *n*-butane will be produced whenever olefin rearrangement is observed. The essential absence of *n*-butane production implies that amorphous solid acids do not promote hydride transfer reactions. Proton transfer between catalyst and butenes must, however, occur since butenes are isomerized by these acids. While Eqs. (1) and (2) suggest that both paraffin and olefin isomerization processes could occur via a common set of C_4 carbonium ion intermediates, the absence of paraffin isomerization indicates that free carbonium ions are not formed on the surface of amorphous solid acids such as SiO_2–Al_2O_3. Polarized intermediates, in which

TABLE 3

Distribution of Butene Isomers Generated from Isobutane[a]

Catalyst	T °K	$\frac{\text{Butene-1 + isobutene}^b}{cis + trans\text{-Butene-2}}$
Blank	923	300
$MgAl_2O_4$	923	200
γ-Al_2O_3	873	7.6
SiO_2–Al_2O_3	873	1.9
0.9% Cl–Al_2O_3	873	1.8
0.9% F–Al_2O_3	823	1.6
Faujasite	773	1.5

[a] Reaction conditions: 101 kPa total pressure, 50 cm^3 *i*-C_4H_{10}/min, 150 cm^3 He/min, 1.0 g catalyst.

[b] Equilibrium values for this ratio vary between 1.40 and 1.44 through the 923 to 773 K temperature range (equilibrium data abstracted from Stull, D. R., Westrum, E. F., and Sinke, G. C., "The Chemical Thermodynamics of Organic Compounds." John Wiley, New York, 1969).

1.
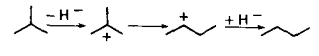

2.
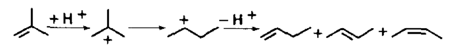

bonding exists between the substrate molecule and the surface, can account both for the occurrence of butene isomerization and the absence of butane isomerization. The formation of several possible polarized surface (alkoxy) intermediates is shown in Eq. (3). Olefin isomerization is envisioned to take place by the rearrangement of alkoxy intermediates followed by proton transfer to the catalyst surface and subsequent release of an isoalkene. Paraffin isomerization, however, requires hydride transfer to a relatively free carbonium ion. Intermolecular hydride transfer occurs most readily when a linear transition state is attainable (*29*). In this transition state, there should be a significant overlap of the breaking C–H bond and the vacant *p*-orbital of a planar carbonium ion. When this is attained, facile, long chain hydride transfer processes are observed (*30*). The polar intermediates depicted in Eq. (3) need not have sufficient cationic character or planarity to accept a hydride ion from a paraffin. In such a case, polarized surface species would not be intermediates in a paraffin isomerization process, but could still function to isomerize olefins. In support of this proposal, many solid and liquid acid systems are known which exclusively catalyze the "less" demanding olefin isomerization reactions (*31*).

3.

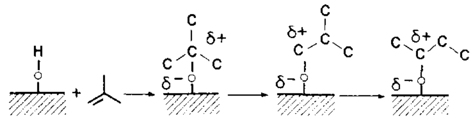

The major conversion products exhibited by an acidic faujasite catalyst are summarized in Table 4. Faujasite is substantially more active than a 1.5% F–Al$_2$O$_3$ catalyst (compare conversions at 773 K). In contrast to the fluorided-alumina catalyst, faujasite readily isomerizes isobutane to *n*-butane. As expected, the selectivity for this skeletal isomerization is favored at lower temperatures. At 773 and 723 K, *n*-butane selectivities are 26 and 39%, respectively. The 1.5% F–Al$_2$O$_3$ catalyst, in comparison, exhibits an *n*-butane selectivity of 4% at 773 K. The ease with which faujasite rearranges isobutane to *n*-butane implies that the acidity of this zeolite catalyst is higher than that of a typical amorphous solid acid. Faujasite produces a substantially lower C$_1$/C$_1$–C$_3$ mole ratio than 1.5% F–Al$_2$O$_3$. From these ratios, it is apparent that faujasite yields five to seven times more C$_3$ products than methane. This pattern indicates that a major fraction of the C$_3$ component arises from a carbonium ion assisted polymerization–rearrangement–cracking sequence of events. As judged by the propane/propene mole ratio, the C$_3$ fraction is highly paraffinic. The overall H/C ratio of the product is essentially the same as the starting isobutane molecule. These results indicate that faujasite, as opposed to amorphous solid acids, facilitates hydride transfer reactions. Hydride transfer also accounts for the low butene yields. Complementary experiments using an isobutene feed showed that butanes are readily generated over faujasite.

TABLE 4

Conversion of Isobutane over Fluorided-Alumina and Faujasite Catalysts[a]

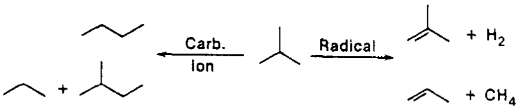

Products (mole%)	Catalyst				
	1.5% F-Al$_2$O$_3$		Faujasite		
(T °K)	823	773	773	773[b]	723
Methane	9.7	1.8	2.5	1.0	0.4
Propene	8.2	2.0	0.9	0.7	0.2
Butenes	9.7	2.8	1.5	0.8	0.7
Propane	1.3	0.3	11.6	2.5	2.7
n-Butane	0.4	0.3	7.9	2.2	4.0
Pentanes	tr	tr	3.9	1.0	1.7
i-Butane	68.5	92.4	69.5	91.2	89.8
Minor	2.2	0.4	2.2	0.6	0.5
H/C ratio	2.23	2.19	2.52	2.48	2.48

[a] Reaction conditions: 101 kPa total pressure, 50 cm^3 *i*-C$_4$H$_{10}$/min, 150 cm^3 He/min, 1.0 g catalyst.

[b] Same reaction conditions as in *a* except 0.3 g of catalyst employed.

TABLE 5

Radical-like Cracking of Isobutane Is Highly Catalyst Dependent

Catalyst	Surface area (m^2/g)	Acidities (μmole/g)[a]			Relative conversion rates[b]		Radical-like cracking[c] (%)
		NH_3	3,5-DMP	2,6-DMP	Total	Radical-like	
Blank	<1	0	—	—	1.0	1.0	100
$MgAl_2O_4$	155	0	—	—	2.2	2.2	100
γ-Al_2O_3	178	295	172	44	35	34	97
SiO_2–Al_2O_3	350	619	279	194	40	38	96
0.9% Cl–Al_2O_3	177	285	185	60	110	108	98
0.3% F–Al_2O_3	179	—	—	—	155	150	96
0.6% F–Al_2O_3	180	—	195	64	240	230	95
0.9% F–Al_2O_3	184	270	195	62	310	290	94
1.5% F–Al_2O_3	184	275	198	83	390	360	92
3.0% F–Al_2O_3	180	—	—	—	270	250	91
5.0% F–Al_2O_3	172	—	—	—	230	205	89
Faujasite	770	1330	1249	1027	2200	730	33

[a] Determined by ammonia (NH_3), 3,5-dimethylpyridine (3,5-DMP), and 2,6-dimethylpyridine (2,6-DMP) adsorption at 523K. NH_3 and 3,5-DMP relate to total acidity while 2,6-DMP estimates Brønsted acidity.

[b] Reaction conditions: 823 K, 101 kPa total pressure, 50 cm^3 i-C_4H_{10}/min, 150 cm^3 He/min, 1.0 g catalyst.

[c] Estimated using the molar product ratio (methane + ethene + propene + butenes)/total conversion products.

Isopentane is the major $C_5(+)$ product formed over faujasite, accounting for better than 85% of the C_5–C_{10} hydrocarbons. At reaction temperatures below 748 K the concentrations of propane and isopentane are comparable. This correspondence suggests that a common reaction intermediate is responsible for their production. A description of the possible form of this intermediate will be presented later. Since only the faujasite catalyst isomerizes isobutane to n-butane or promotes hydride transfer reactions to an appreciable extent, ranking of the solid acids employed in the present study by the parameters presented in Table 1 is not possible. Information obtained from the conversion of isobutane has nevertheless been of substantial importance, particularly in showing that as a class solid acids catalyze the radical-like cracking of isobutane. This type of catalysis has not been widely appreciated. Quantification of the relative radical-like cracking activities of 10 solid acids is presented in the following section.

Radical-like Cracking Activities of Solid Acids

The relative total isobutane conversion rates of 10 solid acids are compared in Table 5. At 823 K, solid acids exhibit total conversion rates 35 to 2200 times faster than a blank reactor. Within the series of solid acids, faujasite is 55 times more active than amorphous SiO_2–Al_2O_3. The total conversion rate exhibited by the nonacidic $MgAl_2O_4$ catalyst is only 2.2-fold higher than the blank reactor. Since the surface area of the mullite beads in the blank reactor is much less than that of the $MgAl_2O_4$ (<1 versus/155 m^2/g), increasing the surface area of a nonacidic catalyst does not significantly enhance cracking. This finding agrees with the studies of Voevodsky (*32*). In marked contrast to faujasite, greater than 90% of the products generated by amorphous solid acids are consistent with a radical-like cracking process. No correlation between catalyst surface area and radical-like cracking activity is apparent. Radical-like cracking also exhibits no direct dependence upon either total catalyst acidity, as measured by ammonia and 3,5-dimethylpyridine adsorption at 523 K or Brønsted acidity, estimated by 2,6-dimethylpyridine adsorption at the same temperature. Amorphous SiO_2–Al_2O_3, for example, exhibits twice the total acidity and three times more Brønsted acid sites than a 1.5% F–Al_2O_3 catalyst, yet fluorided-alumina is a 10-fold more active isobutane cracking catalyst than SiO_2–Al_2O_3. Thus, radical-like cracking must depend upon catalyst properties not directly associated with surface acidity. One such property might be the ability of solid acids to oxidize paraffins to radical-cation intermediates (*25*).

Since free-radical cracking of paraffins is generally thought to be a homogeneous, gas phase process the catalysis of radical-like cracking by solid acids suggests that the surface of these materials is aiding the homolytic cleavage of C–C and C–H bonds. The formation of radical species on the surface of solid acids has in a number of cases been shown to involve molecular oxygen as an electron acceptor (*33–35*). The inadvertent participation of oxygen in our studies was investigated by converting isobutane over amorphous solid acids in the presence of added oxygen. The major results of these studies are summarized in Table 6. Added oxygen enhanced the total isobutane conversion rate of the blank reactor by a factor of 1.2. The small rate enhancement caused by oxygen agrees with reported thermal cracking studies (*8, 36*). Product selectivities were not altered by the addition of oxygen. Thus, for the blank reactor, the homogeneous, gas phase decomposition of isobutane is aided slightly by the presence of oxygen, presumably through the formation of peroxide intermediates (*37*). In contrast to the blank reactor, the rates of conversion of isobutane over two amorphous solid acids decreased 40 to 50% upon oxygen addition. Since coke makes decreased in the presence of oxygen, lowered isobutane conversion rates would not be expected if the main role of oxygen was to maintain a clean catalyst surface. The lowered conversion rates suggest then that radical-like intermediates generated on the surface of these solid acids are sequestered by oxygen. This suggestion is reasonable, since molecular oxygen is known to inhibit numerous radical reactions (*38*).

The Effect of Water on the Conversion of Isobutane over Solid Acids

The addition of water to cracking catalysts has been widely reported to increase the rates of decomposition of numerous hydrocarbons (*39–41*). Water addition is

TABLE 6

The Effect of Added Oxygen on the Rates of Conversion of Isobutane[a]

Catalyst	i-C_4H_{10}/O_2 (mole ratio)	T (°K)	Conversion (mole%)	Rates (mole/hr/g × 10^3)					Coke (%)
				C_1	C_1–C_3	$C_4^=$	n-C_4	Total	
Blank	—	923	4.4	0.6	2.4	3.5	—	5.9	—
	330	923	5.4	0.7	3.0	4.2	—	7.2	—
SiO_2–Al_2O_3	—	873	7.1	0.5	2.5	6.6	0.3	9.5	0.08
	330	873	3.8	0.3	1.3	3.6	0.2	5.1	0.05
0.9% F–Al_2O_3	—	823	19.2	2.7	11.4	13.1	0.4	25.7	0.16
	330	823	10.9	1.4	6.5	7.4	0.2	14.6	0.13

[a] Reaction conditions: 101 kPa total pressure. 50 cm^3 i-C_4H_{10}/min, 150 cm^3 He (or 0.1% O_2/He)/min, 1.0 g catalyst.

TABLE 7

The Effect of Added Water on the Rates of Conversion of Isobutane[a]

Catalyst	i-C_4H_{10}/H_2O (mole ratio)	T (°K)	Conversion (mole%)	Rates (mole/hr/g × 10^3)					
				C_1	C_1–C_3	$C_4^=$	n-C_4	$C_5(+)$	Total
SiO_2–Al_2O_3	—	873	4.3	0.5	1.8	3.9	—	—	5.7
	42	873	1.6	0.2	0.9	1.2	—	—	2.1
0.9% Cl/γ-Al_2O_3	—	873	17.2	3.0	11.6	11.0	—	0.4	23.0
	42	873	4.5	0.8	3.1	2.9	—	—	6.0
0.9% F/γ-Al_2O_3	—	823	16.9	2.8	11.3	10.7	0.4	0.2	22.6
	42	823	3.3	0.6	2.4	2.0	—	—	4.4
Faujasite	—	773	25.5	1.0	16.8	1.6	10.9	4.8	34.1
	42	773	20.3	0.9	12.8	1.5	9.4	3.5	27.2

[a] Reaction conditions: 101 kPa total pressure, 50 cm^3 i-C_4H_{10}/min, 150 cm^3 He (or 0.8% H_2O/He)/min, 1.0 g catalyst.

thought to enhance cracking by increasing the number of Brønsted acid sites. The effect of water on the isobutane conversion patterns of four solid acids is summarized in Table 7. Without exception, added water decreased the rates of conversion of isobutane. The quantity of water supplied during a 10-min pulse (530 μmole) is comparable to the molar acid site concentration of the solid acids present in the reactor. Product selectivities over the three amorphous solid acids, as well as the faujasite catalyst, were not significantly altered by the presence of water. The systematic decrease in catalyst activity without major changes in product selectivity upon water addition indicates that water functions as a competitive adsorbent which lowers the concentration of adsorbed hydrocarbon species on the surface of the catalyst.

The Effect of Isobutane Partial Pressure on the Conversion of Isobutane over Solid Acids

The effect of isobutane partial pressure on the total conversion rates of isobutane

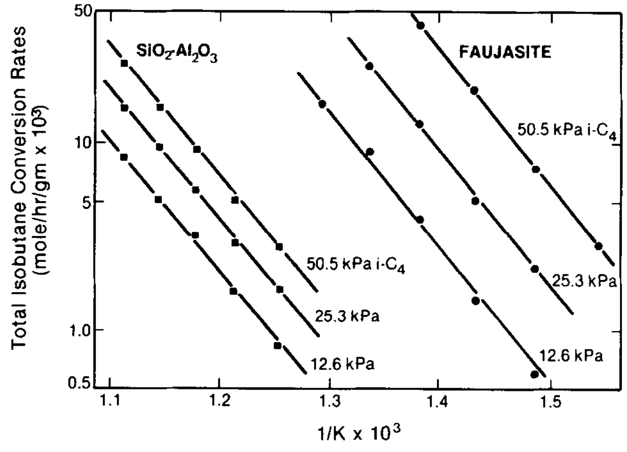

FIG. 3. Effect of isobutane partial pressure on the rates of conversion of isobutane. Reaction conditions: 101 kPa total pressure, i-C_4H_{10}/He (200 cm^3/min), 1.0 g catalyst.

TABLE 8

The Effect of Isobutane Partial Pressure on Conversion Rates[a]

Catalyst	i-C_4H_{10} (kPa)	T (°K)	Conversion (mole%)	Rates (mole/hr/g × 10^3)					
				C_1	C_1–C_3	$C_4^=$	n-C_4	C_5(+)	Total
SiO_2–Al_2O_3	12.6	873	7.5	0.2	1.2	3.7	0.1	—	5.0
	25.3	873	7.1	0.5	2.5	6.6	0.3	0.1	9.5
	50.5	873	5.7	0.9	4.4	10.1	0.6	0.2	15.3
Faujasite	12.6	723	6.0	0.1	1.2	0.5	1.5	0.8	4.0
	25.3	723	9.5	0.2	3.3	0.9	5.4	3.1	12.7
	50.5	723	15.6	0.4	11.0	1.8	18.2	10.8	41.8

[a] Conditions: 101 kPa total pressure, i-C_4H_{10}/He (200 cm^3/min), 1.0 g catalyst.

over amorphous SiO_2–Al_2O_3 and faujasite is summarized in the Arrhenius plots shown in Fig. 3. SiO_2–Al_2O_3 exhibited total conversion rates which doubled upon increasing the isobutane partial pressure by a factor of two. Faujasite, in contrast, displayed total conversion rates which increased by a factor of nearly four upon doubling the partial pressure of isobutane. The differences in the pressure dependencies are amplified in Table 8 where individual isobutane conversion rates over SiO_2–Al_2O_3 and faujasite at three isobutane partial pressures are contrasted.

Isobutane partial pressure dependencies along with the apparent activation energies for the formation of selected isobutane reaction products are summarized in Table 9. SiO_2–Al_2O_3 exhibits isobutane partial pressure dependencies which range from 0.8 to 1.0. The first-order isobutane pressure dependency found for SiO_2–Al_2O_3 agrees with published results (*25*). The faujasite catalyst, with the exception of the methane and butene formation rates, demonstrates a second-order dependence on isobutane. A recent paper by Hilaireau describes a similar second-order dependence for the conversion of isobutane over H-mordenite (*42*). Insight into the mechanism operating over faujasite can be gained by considering Fig. 4 in which the relative propane/isopentane rate ratios at three isobutane partial pressures are plotted against reaction temperature. At lower temperatures and higher isobutane partial pressures, the rates of formation of propane and isopentane are equivalent. This correspondence indicates that these products result from the decomposition of a C_8 intermediate. The generation of a C_8 intermediate, presumably by the alkylation of a C_4 olefin and a C_4 paraffin, is favored at low temperatures and higher isobutane partial pressures. At higher reaction temperatures the increased propane/isopentane rate ratio most likely results from unimolecular cracking of isobutane.

TABLE 9

Summary of Isobutane Partial Pressure Effects

Product	Isobutane dependence[a]		E_a (kcal/mole)	
	SiO_2–Al_2O_3	Faujasite	SiO_2–Al_2O_3	Faujasite
Methane	1.0	1.0	40	42
Propene (ane)	1.0	1.8	36	44
Butenes	0.8	1.0	30	29
n-Butane	1.0	1.9	35	29
Isopentane	—	2.0	—	46
Total	0.9	1.9	33	35

[a] Isobutane dependence refers to the value of the exponent in the expression: rate = $k[i\text{-}C_4H_{10}]^x$ where k is the rate constant for the particular conversion.

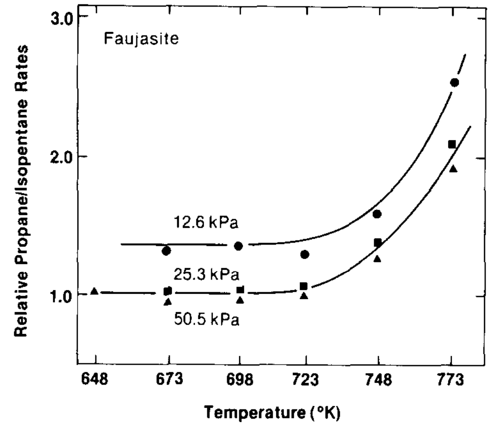

FIG. 4. Relative propane/isopentane formation rates over faujasite. Reaction conditions: 101 kPa total pressure, i-C_4H_{10}/He (200 cm^3/min), 1.0 g catalyst.

The differences in kinetics are rationalized by the mechanistic considerations of the next section. Anticipating that discussion, we note that the distinction between catalysts appears to depend on the ability of a solid acid to generate chain carrying carbonium ion intermediates. If it does, a second-order dependence on isobutane pressure is found, if not, a first-order process results.

Speculations on the Mechanism of Isobutane Conversion over Solid Acids

A mechanism for the conversion of isobutane over solid acids must account for (1) the radical-like catalysis exhibited by all solid acids, (2) the absence of carbonium ion initiated reactions over amorphous solid acids, and (3) the second-order isobutane pressure dependency exhibited by an acidic faujasite. A simple kinetic model consistent with the above observations can be developed by assuming the existence of carbonium ion chain reactions. Using a steady-state model which has been widely employed to describe polymerization kinetics, as well as the conversion of alkanes in sulfuric acid, the data may be rationalized (*43–45*). The steady-state model is composed of three distinct steps, namely, initiation, propagation, and termination. These steps will be treated individually for the isobutane–solid acid systems.

Initiation Step

The initiation step is proposed to be the generation of a radical cation which ultimately leads to the formation of olefins. Isobutene formation is assumed to occur by the decomposition of a surface bound isobutane radical cation. A surface bound radical cation is envisioned to be formed by the one-electron oxidation of isobutane by an electron acceptor site (EA) on the surface of solid acids. Although no definitive experimental proof exists at this time, electron acceptor sites may be associated with electron deficient oxygen atoms on the surface of solid acids (*46*). Equation (4) suggests

$$i\text{-}C_4H_{10} + EA \xrightarrow{k_i} [i\text{-}C_4H_{10}^{\ddagger}][EA^{\cdot}] \qquad (4)$$

that the ease of electron transfer from isobutane to a solid acid is dependent upon the oxidizing ability of the solid. Thus, k_i would be expected to be subject to catalysis by solid acids of varying oxidizing power. Based upon the known decomposition pathways of gas phase radical cations, a surface bound isobutane radical cation is assumed to decompose by the routes shown in Eq. (5). The predicted products readily account for the radical-like

$$[i\text{-}C_4H_{10}^{\ddagger}][EA^{\cdot}] \begin{cases} \xrightarrow{k_1} i\text{-}C_4H_8 + H_2 + EA \\ \xrightarrow{k_2} C_3H_6 + CH_4 + EA \end{cases} \qquad (5)$$

catalysis displayed by all the solid acids investigated in these studies. Using the stable methane product as a marker, the k_1/k_2 rate ratio averaged near two over the nine amorphous solid acids studied. Subsequent reactions of the primary isobutene and propene products, however, are markedly different over amorphous solid acids and faujasite. Amorphous solid acids do not promote reactions typically expected of carbonium ion intermediates, e.g., hydride transfer reactions. Only isomerization of isobutene occurs, presumably via the polar surface bound intermediates suggested in Eq. (3). Thus conversion of isobutane over amorphous solid acids is limited to the radical-like products predicted by Eq. (5).

Faujasite, however, readily catalyzes hydride transfer and alkylation reactions. The facile catalysis of these reactions strongly indicates that essentially free C_4 carbonium ions are generated by the zeolite. The most stable carbonium ion produced by the transfer of a proton from faujasite to isobutene is the tertiary C_4 cation (*47*). This protonation is shown in Eq. (6) where HY represents faujasite. Faujasite produces

$$i\text{-}C_4H_{8(ad)} + HY \overset{K}{\rightleftarrows} t\text{-}C_4H_9^+ + Y^- \qquad (6)$$

little free hydrogen, thus, redistribution of hydrogen generated by pathway k_1 of Eq. (5) must take place. Since substantial quantities of *n*-butane and propane are generated over faujasite, hydrogen incorporation may occur in part by the routes outlined in Eqs. (7) and (8) (*47*). Equations (7) and (8) not only

$$i\text{-}C_4H_8 \xrightarrow{H^+} t\text{-}C_4H_9^+ \rightarrow$$

$$s\text{-}C_4H_9^+ \xrightarrow{H_2} n\text{-}C_4H_{10} + H^+ \qquad (7)$$

$$C_3H_6 \xrightarrow{H^+} C_3H_7^+ \xrightarrow{H_2} C_3H_8 + H^+ \qquad (8)$$

account for the redistribution of hydrogen but also rationalize the low yields of butenes and propene displayed by faujasite.

Termination Step

Termination of carbonium ion initiated reactions over faujasite is assumed to result from the loss of adsorbed isobutene to the gas phase (Eq. (9)).

$$i\text{-}C_4H_{8(ad)} \xrightarrow{k_t} i\text{-}C_4H_{8(g)} \qquad (9)$$

Steady-State Approximation

In the steady-state approximation, the rates of initiation and termination steps are assumed to be equal. Equation (10) results from equating these steps.

$$k_i[C_4H_{10}][EA] = k_t[i\text{-}C_4H_8]_{(ad)} \qquad (10)$$

Solving for $[i\text{-}C_4H_8]_{ad}$ in Eq. (6) and substituting this relationship into Eq. (10) yields the expression given in Eq. (11).

$$k_i[i\text{-}C_4H_{10}][EA] = \frac{k_tK[t\text{-}C_4H_9^+][Y^-]}{[HY]} \qquad (11)$$

Propagation Step

The equation used to describe the rate of propagation is shown in Eq. (12). The form of this equation is similar to that used in the

$$R_p = k_p[i\text{-}C_4H_{10}][t\text{-}C_4H_9^+] \qquad (12)$$

description of many chain reactions noted earlier (*43–45*). Substituting into Eq. (12) the relationship for $[t\text{-}C_4H_9^+]$ obtained from Eq. (11) produces the final expression given in Eq. (13). Assuming that the surface concentration of

$$R_p = \frac{k_pk_i[i\text{-}C_4H_{10}]^2[EA][HY]}{k_tK[Y^-]} \qquad (13)$$

isobutane is directly related to its bulk partial pressure, Eq. (13) indicates that the rate of propagation of carbonium ion reactions is proportional to the square of the isobutane partial pressure. This prediction is in agreement with the kinetics of isobutane conversion over faujasite. Equation (13) also suggests that the rate of carbonium ion initiated reactions are not only dependent upon the Brønsted acid strength but also are dependent upon the electron acceptor ability (oxidizing power) of faujasite. The preceding model may be applied to the amorphous solid acids as well as to the acidic faujasite. The model suggests that nearly all of the products derived from the amorphous acids comes from Eq. (5), the cracking of a surface adsorbed radical cation. The variation of activity with these substances is primarily attributed to the ability of the acid to generate radical cations by oxidizing isobutane. Studies cur-

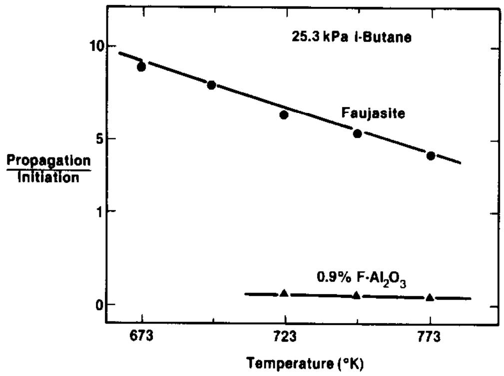

FIG. 5. Effect of temperature on the propagation/initiation rate ratio. Reaction conditions: 101 kPa total pressure, 50 cm^3 i-C_4H_{10}/min, 150 cm^3 He/min, 1.0 g catalyst. Propagation/initiation rate ratio estimated from the product ratio [propane + n-butane + isopentane]/3[CH_4].

rently underway in these laboratories are addressing the effects changes in the electron acceptor ability of solid acids have upon the carbonium ion activities of these materials. Preliminary results are consistent with the predictions of Eq. (13).

An estimate of the chain length or number of carbonium ion assisted propagation reactions per initiation reaction is obtained by using the product ratio [propane + n-butane + isopentane]/3[CH_4]. The numerator constitutes the principle carbonium ion products while the methane concentration in the denominator reflects the radical initiation step. The factor 3 in the denominator results from the rate relationship between paths k_1 and k_2 in Eq. (5). This ratio plotted against temperature is shown in Fig. 5. Faujasite exhibits 5 to 10 propagation reactions for each initiation reaction. As expected, the carbonium ion assisted propagation reactions became less favorable at higher reaction temperatures. A 0.9% F–Al_2O_3 catalyst by way of comparison exhibits propagation/initiation ratios less than 0.1. Thus for all practical purposes, the fluorided-alumina catalyst is devoid of carbonium ion reactions. Although the propagation/initiation ratios demonstrated by faujasite are low when contrasted with sulfuric acid catalyzed reactions of alkanes (*44*) (typical propagation/initiation ratios in sulfuric acid range between 100 and 1000 at 300 K), the occurrence of carbonium ion reactions at 700–800 K is indeed remarkable.

4. CONCLUSIONS

1. Amorphous solid acids, such as SiO_2–Al_2O_3, γ-Al_2O_3, and halided-Al_2O_3, exhibit isobutane cracking products which are consistent with those expected from the decomposition of radical-cation intermediates. Essentially no isomerization of isobutane to n-butane occurs over amorphous solid acids.
2. The extent of radical-like cracking is highly dependent upon the particular amorphous solid acid employed. The basis for the catalysis of radical-like cracking appears to be related to the oxidizing power of the solid acid and not acid strength.
3. Faujasite, in contrast, cracks, isomerizes, and polymerizes isobutane by a combination of radical-like and carbonium ion routes. The formation of isobutene by a radical-like route is a prerequisite for subsequent carbonium ion reactivity. An outstanding attribute of the acidic faujasite is its ability to catalyze intermolecular hydride transfer reactions which are all but missing over amorphous solid acids.
4. Based upon the above statements, faujasite is considered to be significantly more acidic than amorphous solid acids.

ACKNOWLEDGMENTS

The authors thank Drs. L. L. Murrell, S. L. Soled, and L. G. Sherman for their interest and helpful discussions during the course of these studies.

REFERENCES

1. Voge, H. H., *in* "Catalysis" (P. H. Emmett, Ed.), Vol. 6. Reinhold, New York, 1958.
2. Gates, B. G., Katzer, J. R., and Schuit, G. C. H., "Chemistry of Catalytic Processes." McGraw-Hill, New York, 1979.
3. Germain, J. E., "Catalytic Conversion of Hydrocarbons." Academic Press, New York, 1969.
4. Pines, H., and Wackher, R. C., *J. Amer. Chem. Soc.* **68**, 595 (1946).

5. Haensel, V., *Advan. Catal.* **3,** 179 (1951).
6. Whitmore, F. C., Ropp, W. S., and Cook, N. C., *J. Amer. Chem. Soc.* **72,** 1507 (1951).
7. Hofmann, J. E., and Schriesheim, A., *J. Amer. Chem. Soc.* **84,** 957 (1962).
8. Greensfelder, B. S., Voge, H. H., and Good, G. M., *Ind. Eng. Chem.* **41,** 2573 (1949).
9. Rice, F. O., *J. Amer. Chem. Soc.* **55,** 3035 (1933).
10. Fabuss, B. M., Smith, J. O., and Satterfield, C. N., *Adv. Pet. Chem. Refining* **9,** 157 (1964).
11. Kossiakoff, A., and Rice, F. O., *J. Amer. Chem. Soc.* **65,** 590 (1943).
12. Appleby, W. G., Avery, W. H., and Meerbott, W. K., *J. Amer. Chem. Soc.* **69,** 2279 (1947).
13. Wolkoff, P., and Holmes, J. L., *J. Amer. Chem. Soc.* **100,** 7346 (1978).
14. Wendelboe, J. F., Bowen, R. D., and Williams, D. H., *J. Amer. Chem. Soc.* **103,** 2333 (1981).
15. Corio, P. L., and Shih, S., *J. Phys. Chem.* **75,** 3475 (1971).
16. Field, F. H., and Franklin, J. L., "Electron Impact Phenomena." Academic Press, New York, 1957.
17. Benesi, H. A., and Winquist, B. H. C., *Adv. Catal.* **27,** 97 (1978).
18. Aldridge, L. P., McLaughlin, J. R., and Pope, C. G., *J. Catal.* **30,** 409 (1973).
19. Frilette, V. J., Weisz, P. B., and Golden, R. L., *J. Catal.* **1,** 301 (1962).
20. Brunauer, S., Emmett, P. H., and Teller, E., *J. Amer. Chem. Soc.* **60,** 309 (1938).
21. Sinfelt, J. H., Hurwitz, H., and Schulman, R. A., *J. Chem. Phys.* **64,** 1559 (1960).
22. Soled, S. L., McVicker, G. B., and DeRites, B., Proceedings, 11th North Amer. Thermal, Anal. Soc., New Orleans, 1981, p. 417.
23. Steacie, E. W. R., and Puddington, I. E., *Canad. J. Res.* **B16,** 176 (1938).
24. Hall, W. K., Lutinski, F. E., and Gerberick, H. R., *J. Catal.* **3,** 512 (1964).
25. Franklin, J. L., and Nicholson, D. E., *J. Phys. Chem.* **60,** 59 (1956).
26. Miale, J. N., Chen, N. Y., and Weisz, P. B., *J. Catal.* **6,** 278 (1966).
27. Chen, N. Y., Proceedings, 5th Int. Congr. Catal., North-Holland, Amsterdam, 1973, p. 1343.
28. Wang, I., Chen, T., Choa, K., and Tsai, T., *J. Catal.* **60,** 140 (1979).
29. Deno, N. C., Peterson, H. J., and Saines, G. S., *Chem. Rev.* **60,** 7 (1960).
30. (a) Mirda, D., Rapp, D., and Kramer, G. M., *J. Org. Chem.* **44,** 2619 (1979). (b) Kramer, G. M., Hudson, B. E., and Melchior, M. T., *J. Phys. Chem.* **71,** 1525 (1967). (c) Bartlett, P. D., Condon, F. E., and Schneider, A., *J. Amer. Chem. Soc.* **66,** 1531 (1944).
31. Condon, F. E., *in* "Catalysis" (P. H. Emmett, Ed.), Vol. 6, p. 43. Reinhold, New York, 1958.
32. Voevodsky, V. V., *Trans. Faraday Soc.* 65 (1959).
33. Hall, W. K., and Dollish, F. R., *J. Colloid Interface Sci.* **26,** 261 (1968).
34. Fogo, J. K., *J. Phys. Chem.* **65,** 1919 (1961).
35. Porter, R. P., and Hall, W. K., *J. Catal.* **5,** 366 (1966).
36. Hazlett, R., *Ind. Eng. Chem. Prod. Res. Dev.* **16,** 175 (1977).
37. Benson, S. W., "Thermochemical Kinetics." Wiley-Interscience, New York, 1964.
38. Gould, E. S., "Mechanism and Structure in Organic Chemistry," p. 693. Holt, Rinehart, New York, 1959.
39. Hinden, S. G., Oblad, H. G., and Mills, G. A., *J. Amer. Chem. Soc.* **77,** 535 (1955).
40. Matsushita, K., and Emmett, P. H., *J. Catal.* **13,** 128 (1969).
41. Hansford, R. C., *Ind. Eng Chem.* **39,** 849 (1947).
42. Hilaireau, P., Bearez, C., Chevalier, F., Perot, G., and Guisnet, M., *Zeolites* **2,** 69 (1982).
43. Benson, S. W., "The Foundations of Chemical Kinetics," p. 601. McGraw-Hill, New York, 1960.
44. Kramer, G. M., *J. Org. Chem.* **32,** 1916 (1967).
45. Kramer, G. M., *J. Org. Chem.* **32,** 920 (1967).
46. Shih, S., *J. Catal.* **79,** 390 (1983).
47. Brouwer, D. M., and Hogeveen, H., *in* "Progress in Physical Organic Chemistry" (H. Streitweiser, Jr. and R. W. Tuft, Eds.), Vol. 9, p. 179. Wiley (Interscience), New York, 1972.